# Magnetic and electronic ground states of B-site-substituted LaMnO 3: From antiferromagnetism to ferromagnetism

B. Vertruyen, Delphine Flahaut, S. Hebert, A. Maignan, Christine Martin, M. Hervieu, B. Raveau

▶ **To cite this version:**

B. Vertruyen, Delphine Flahaut, S. Hebert, A. Maignan, Christine Martin, et al.. Magnetic and electronic ground states of B-site-substituted LaMnO 3: From antiferromagnetism to ferromagnetism. Journal of Magnetism and Magnetic Materials, 2004, 280 (1), pp.75-83. 10.1016/j.jmmm.2004.02.023 . hal-01499387

**HAL Id: hal-01499387**
**https://hal.science/hal-01499387**

Submitted on 16 Mar 2021

**HAL** is a multi-disciplinary open access archive for the deposit and dissemination of scientific research documents, whether they are published or not. The documents may come from teaching and research institutions in France or abroad, or from public or private research centers.

L'archive ouverte pluridisciplinaire **HAL**, est destinée au dépôt et à la diffusion de documents scientifiques de niveau recherche, publiés ou non, émanant des établissements d'enseignement et de recherche français ou étrangers, des laboratoires publics ou privés.

**Title :**
Magnetic and electronic ground-states of B-site-substituted $LaMnO_3$ :
from Antiferromagnetism to Ferromagnetism

**Authors :**

B. Vertruyen[1]*, D. Flahaut[2], S. Hébert[2], A. Maignan[2], C. Martin[2], M. Hervieu[2], B. Raveau[2]

[1] LCIS/SUPRATECS, Chemistry Institute B6, University of Liège, Sart-Tilman, B-4000 Liège, Belgium
[2] Laboratoire CRISMAT, UMR 6508 associée au CNRS, ISMRA, 6 Bd Maréchal Juin, 14050 Caen Cedex, France

* Corresponding author :
e-mail : b.vertruyen@ulg.ac.be, phone : + 32 4 3663452, fax : + 32 4 3663413

**ABSTRACT**

We report about the physical properties of samples obtained by different substitutions on the Mn site of $LaMnO_3$ : $LaMn_{0.85}Ni_{0.15}O_3$, $LaMn_{0.85}Ga_{0.15}O_3$ and $LaMn_{0.5}Ga_{0.5}O_3$. It is well known that the antiferromagnetic orbitally-ordered ground-state of $LaMnO_3$ is easily destroyed to give way to ferromagnetism. However, this ferromagnetic behaviour can result from several mechanisms : depending on the nature of the substituting cation and on the substitution level, the physical properties derive from a complex interplay between exchange interactions, orbital ordering and Jahn-Teller distortion. As a result, there are noticeable differences between the physical properties of the different samples, even though all three samples display a ferromagnetic component in zero applied magnetic field. In this paper we compare the crystallographic, electrical and magnetic properties of these samples, with a special attention for the AC susceptibility behaviour.

**PACS**

75.30.Et; 75.50.Dd, 75.60.-d

**KEYWORDS**

Manganites, magnetic structure, exchange interactions, AC susceptibility

## INTRODUCTION

Since the early nineties, there has been a renewed interest for the rare earth manganites with perovskite structure, due to the discovery of Colossal MagnetoResistance (CMR) in some compounds of this family [1,2]. A remarkable property of these materials is the possibility to induce ferromagnetism by cationic substitutions on the different sites of the antiferromagnetic parent compound $LnMnO_3$ [3]. The most famous illustration of this mechanism is the substitution of alkaline-earth ions such as $Ca^{2+}$ or $Sr^{2+}$ on the A site of $LaMnO_3$, which can lead to the appearance of a paramagnetic-ferromagnetic transition coupled to high magnetoresistance ratios [3,4]. However substitutions on the Mn site are also very interesting, from a theoretical point of view, due to the prominent role played by the manganese-oxygen network in the physics of these materials [5,6]. Introducing foreign cations on the Mn site of mixed-valent manganites $Ln_{1-x}A_xMnO_3$ is known to lead to severe modifications of the physical properties, as well in conductive ferromagnetic manganites [7-9] as in insulating charge-ordered compounds [10,11]. The single-valent parent compound $LaMnO_3$ is also very sensitive to Mn-site substitution [6,12,13] (as well as to any other type of modification : A-site substitution [14,15] or oxygen non-stoichiometry [16-18]). The antiferromagnetic orbitally-ordered state of $LaMnO_3$ is easily destroyed to give way to ferromagnetism. However, this ferromagnetic behaviour can result from several mechanisms : depending on the nature of the substituting cation and on the substitution level, the physical properties derive from a complex interplay between exchange interactions, orbital ordering and Jahn-Teller distortion [19-21].

In this paper we deal with the physical properties of samples obtained by different substitutions on the Mn site of $LaMnO_3$ : $LaMn_{0.85}Ni_{0.15}O_3$, $LaMn_{0.85}Ga_{0.15}O_3$ and $LaMn_{0.5}Ga_{0.5}O_3$. Since $Ga^{3+}$ is isovalent to $Mn^{3+}$, Ga-susbtituted manganites are often used as a model system for studying super-exchange interactions [22-25]. On the contrary, substitution by $Ni^{2+}$ leads to the appearance of $Mn^{4+}$ species and to double exchange interactions between $Mn^{3+}$ and $Mn^{4+}$ ions [26-29]. Besides, contrary to $Ga^{3+}$ ($d^{10}$), the $Ni^{2+}$($d^8$) ion can be involved in exchange interactions through its unpaired $e_g$ electrons. As a result of these different physical mechanisms, there are noticeable differences between the physical properties of the different samples, even though all three samples display a ferromagnetic component in the absence of applied magnetic field. In the following we will review and compare the crystallographic, electrical and magnetic properties of these samples, with a special attention for the AC susceptibility behaviour.

## EXPERIMENTAL

Samples of $LaMnO_3$, $LaMn_{0.85}Ni_{0.15}O_3$ and $LaMn_{1-x}Ga_xO_3$ (with x = 0.15 and 0.5) were prepared by solid-state reaction at high temperature (1250°C for 48 h). Stoichiometric amounts of the appropriate oxides ($La_2O_3$, $Mn_2O_3$, $MnO_2$, NiO, $Ga_2O_3$) were pressed into bars after a thorough grinding, put into small alumina crucibles and

sealed into evacuated silica tubes. In the case of the $Ni^{2+}$-substituted sample it was necessary to use a mixture of $Mn_2O_3$ and $MnO_2$ in order to obtain the "$O_3$" stoichiometry.

X-ray powder diffraction patterns were collected at room temperature for 2θ between 15° and 80° in steps of 0.02° on a Philips diffractometer (Cu $K_\alpha$ radiation). Rietveld refinement of the diffractograms was carried out in the Pnma space group with the Fullprof software.

The powders (except the $LaMn_{0.5}Ga_{0.5}O_3$ sample) were also characterised by neutron diffraction as a function of temperature at the Leon Brillouin Laboratory (Saclay, France). Details of these experiments will be published elsewhere [30].

Numerous crystallites of the different compounds were characterized by electron diffraction (ED) and Energy Dispersive Spectroscopy (EDS) in a JEOL 200CX transmission electron microscope, equipped with a KEVEX analyser.

DC magnetic measurements were performed with a Quantum Design SQUID. AC susceptibility properties were measured under 1 mT for frequencies ranging between 100 and 10000 Hz with a Quantum Design susceptometer.

The electrical resistivity under 0 and 7 T was measured by the four-point method with a Quantum Design Physical Property Measurement System (PPMS). The thermopower measurements were also carried out in the PPMS system, using a home-made sample holder based on a four-point steady-state method with separate measuring and power contacts.

## RESULTS

### Chemical and structural characterisations

By EDS analysis, all samples were found to be pure and displayed a homogeneous cationic distribution in the limit of the technique accuracy. The $Mn^{4+}$ content of each sample was estimated by thermopower measurements. When comparing the thermopower values at 300 K (see Table 1) with data published by Töpfer et al. [16] for the $LaMnO_{3+\delta}$ series, it appears that the $LaMnO_3$, $LaMn_{0.85}Ga_{0.15}O_3$ and $LaMn_{0.85}Ni_{0.15}O_3$ samples compare well with $LaMnO_{3+\delta}$ samples containing respectively 0%, 4% and 12% $Mn^{4+}$. Thermopower could not be measured for the 50%-substituted sample due to the large resistivity of this material.

The X-ray diffraction patterns of all samples are shown in Figure 1. Each pattern displays the characteristic peaks of a single-phase perovskite manganite structure and can be indexed in the Pnma space group by Rietveld refinement. Note that the Pnma space group was confirmed by electron diffraction experiments.

The cell parameters are shown in Figure 2. The lattice parameters for $LaMnO_3$ are in good agreement with the results obtained by Hauback et al. [31] for their stoichiometric $LaMnO_3$ ORT1 phase. Substitution by $Ga^{3+}$ or $Ni^{2+}$ on the Mn site leads to a decrease of the cell volume. The O'-type distortion of the orthorhombic cell ($b/\sqrt{2} < c < a$) [32] remains significant in the case of the 15%$Ga^{3+}$ substitution but becomes very small for the samples substituted by 50% $Ga^{3+}$ or 15 % $Ni^{2+}$.

## Neutron diffraction

Neutron diffraction patterns were collected as a function of temperature for the $LaMnO_3$, $LaMn_{0.85}Ga_{0.15}O_3$ and $LaMn_{0.85}Ni_{0.15}O_3$ samples. The detailed analysis of these experiments will be published elsewhere [30]. Only the results concerning the magnetic structure are mentioned here. $LaMnO_3$ displays an A-type antiferromagnetic order, which disappears between 135 and 140 K. In the case of the $LaMn_{0.85}Ga_{0.15}O_3$ sample, the same antiferromagnetic structure coexists with a long-range ferromagnetic component. Both magnetic orders seem to disappear at ~105 K, but there is a significant uncertainty concerning the temperature where the ferromagnetic component vanishes, due to the small intensity of the signal. The ferromagnetic and antiferromagnetic moments at 1.4 K are refined to 1.8 and 3.5 $\mu_B$/Mn respectively. The $LaMn_{0.85}Ni_{0.15}O_3$ sample exhibits a ferromagnetic long-range order below ~ 160 K. The pattern of the $LaMn_{0.5}Ga_{0.5}O_3$ sample was not collected, since the long-range ferromagnetic order of this compound had already been established by the neutron diffraction study of Cussen et al. [33].

## AC magnetic properties

Figure 3 shows the temperature dependence of the AC susceptibility in-phase component for $LaMnO_3$ and the gallium-substituted samples ($\mu_0 H_{AC}$ = 1 mT, f = 100, 1000 and 10000 Hz). The out-of-phase component displays a similar behaviour and is therefore not shown here.

A distinct peak can be seen in each curve of in-phase susceptibility, but in the case of the $LaMn_{0.85}Ga_{0.15}O_3$ sample, there is a shoulder on the low-temperature side of the main peak. When the gallium substitution level is increased from 0 to 50 %, (i) the peak temperature decreases from 134 K to 57 K, (ii) the peak becomes broader, and (iii) both the susceptibility value at the peak and the low-temperature susceptibility increase.

Figure 3 also shows the influence of the frequency of the AC magnetic field on the magnetic susceptibility. This is often parameterised by the quantity $K = \Delta T_p/(T_p \Delta(\log f))$, where $T_p$ is the peak temperature and f the frequency of the AC magnetic field [34]. In the case of $LaMnO_3$, the variation is not significant. In the case of the gallium-substituted samples, the temperature of the susceptibility maximum is slightly increased when the frequency increases : K ~ $5.10^{-3}$ and $7.10^{-3}$ for the 15%Ga- and 50%Ga-substituted samples respectively.

The $LaMn_{0.85}Ni_{0.15}O_3$ sample displays a different behaviour. The temperature dependences of the in-phase ($\chi'$) and out-of-phase ($\chi''$) components of the AC susceptibility are shown in figure 4 ($\mu_0 H_{AC}$ = 1 mT, f = 100 and 1000 Hz). When the temperature is decreased, $\chi'$ shows a sharp ferromagnetic transition at 157 K, followed by a smooth decrease down to about 100 K, where the susceptibility drops by approximately 60 %. Below 60 K, $\chi'$ remains almost constant. The influence of the frequency of the AC magnetic field is significant only in the temperature range corresponding to the susceptibility drop (*i.e.* between 60 and 100 K).

Both the ferromagnetic transition and the susceptibility drop correspond to peaks in the out-of-phase susceptibility curve. The low temperature peak is shifted to a higher temperature when the frequency of the AC magnetic field is increased (K ~ $8.10^{-2}$).

## DC magnetic properties

Figure 5 presents the dependence of the magnetic moment at 5 K as a function of the DC magnetic field. The magnetic moment values are given in $\mu_B$/formula unit. The magnetisation at 5 T, the coercive field and the remnant magnetisation of the different samples are collected in Table 1. In the case of Ga substitution, the magnetisation can also be expressed in $\mu_B$/Mn, since $Ga^{3+}$ ions have a $d^{10}$ configuration and do not contribute to the magnetic moment.

The $LaMnO_3$ compound displays a small magnetic moment at 5 T (0.37 $\mu_B$) and a large magnetic hysteresis. Ga substitution induces both a decrease of the magnetic hysteresis and an increase of the magnetic moment. The 15%Ga-substituted sample shows a magnetisation of 1.56 $\mu_B$/Mn at 5 T with a hysteresis that is still significant. In the case of the 50%Ga-substituted sample, the magnetisation reaches 3.7 $\mu_B$/Mn, close to the theoretical spin-only value of 4 $\mu_B$/Mn, while the coercive field decreases by one order of magnitude. Ni substitution has a much more pronounced influence than Ga substitution : for a 15% substitution, the hysteresis is drastically suppressed and the magnetisation reaches 3.5 $\mu_B$/formula unit.

Figure 6 display the first-magnetisation curves at 5 K for $LaMn_{0.85}Ga_{0.15}O_3$ and $LaMn_{0.85}Ni_{0.15}O_3$. The $LaMn_{0.85}Ga_{0.15}O_3$ sample presents a "S-shape" curve : the magnetisation increases slowly up to a field H* ($\mu_0$H* ~ 0.3 T, as indicated by an arrow in figure 6) where the slope of the m(H) curve becomes noticeably sharper. A similar behaviour is observed for the $LaMnO_3$ and $LaMn_{0.5}Ga_{0.5}O_3$ samples, with $\mu_0$H* = 0.1 T and 0.035 T respectively. On the contrary, the $LaMn_{0.85}Ni_{0.15}O_3$ curve (inset fig. 6) does not present this behaviour, within the measurement precision ($\mu_0$H* would be below 0.01 T).

## Transport properties

All samples display an insulating behaviour in the temperature range where the electrical resistance does not exceed the measuring limit of the device (figure 7). No significant magnetoresistance is observed in the case of the undoped and Ga-substituted samples. But it must be stressed that their magnetic transition temperature is outside the temperature range where the resistivity measurement was possible. On the contrary, in the case of the 15%Ni-substituted sample, the temperature dependence of the magnetoresistance displays a peak at 170 K, with a $(R_{0T} - R_{7T})/R_{7T}$ value of 37 %.

Table 1 summarises for each sample (i) the resistivity value at 350 K and (ii) the $E_a$ value obtained by fitting the experimental data with an exponential law $R \propto \exp(-E_a/kT)$. In the case of the 15%Ni-substituted sample, distinct $E_a$ values are observed below and above 170 K. Compared with the values for $LaMnO_3$, both $E_a$ and the resistivity at 350 K tend to increase with gallium substitution and decrease with nickel substitution. Comparing the 15% substitutions, the modifications are much more pronounced for nickel substitution than for gallium substitution.

## DISCUSSION

The whole set of properties measured for our reference $LaMnO_3$ sample compares well with literature data for oxygen-stoichiometric material, as well for crystallographic parameters [31] as for electrical transport and magnetic measurements [16,34,36,37]. Similarly to other authors [31,36,37], we observed the appearance of a small but significant ferromagnetic moment when a magnetic field is applied. Even though it cannot be ruled out that this signal results from a very small amount of $Mn^{4+}$, the systematic occurrence of this weak ferromagnetic component throughout the literature is disconcerting, and some authors have proposed that the magnetic ground state of $LaMnO_3$ might present a small canting of the manganese spins [31,37]. In this respect, it is interesting to note the slope change at $\mu_0 H^* \sim 0.1$ T in the first magnetisation curve, and more generally the magnetic hysteresis that affects the whole m(H) curve.

The Néel temperature is characterized by a peak in the temperature dependence of the in-phase susceptibility of $LaMnO_3$. Indeed the antiferromagnetic-to-paramagnetic transition corresponds to the temperature range where the spins become free to rotate and to adopt a disordered paramagnetic state. Below $T_N$, the susceptibility decreases when the temperature decreases, as a result of the antiferromagnetic order, which hinders the spin movements [36].

When the manganese site is substituted by gallium ions, the $Mn^{3+}$-$Mn^{3+}$ interactions are "diluted" by the non-magnetic $d^{10}$ $Ga^{3+}$ ions. Besides, the crystallographic data indicate that gallium substitution tends to decrease the orthorhombic distortion of the perovskite structure. This is usually considered as the sign that the long range Jahn-Teller structural order progressively disappears [32]. As a result, the orbital ordering of the $e_g$ $Mn^{3+}$ orbitals and the A-type antiferromagnetic ordering of the manganese spins are destabilised.

For a 15%-$Ga^{3+}$ substitution, neutron diffraction results show that a long-range ferromagnetic component ($\mu_{FM} \sim 1.8\ \mu_B$/Mn) is present in the magnetic ground state of the compound and coexists with the A-type antiferromagnetic order. At the present stage, it is not possible to decide whether the magnetic ground-state corresponds to a canted magnetic order or to a mixture of ferromagnetic and antiferromagnetic zones resulting from a phase separation mechanism [38,39]. The application of a magnetic field results in an increase of the magnetic moment up to 1.65 $\mu_B$/Mn at 5 T. It must be stressed here that the 4 % parasite $Mn^{4+}$ ions detected in the sample during the chemical characterisation cannot account for this magnetic moment value, as confirmed by comparison with literature data for $LaMnO_{3.025}$ [37]. However it cannot be ruled out that the shoulder to the in-phase susceptibility peak in the $\chi'(T)$ curve might be an artefact resulting from these $Mn^{4+}$ ions, since the shoulder corresponds to less than 10% of the total signal at a given temperature. Therefore only the behaviour of the main peak will be discussed here. Contrary to the case of $LaMnO_3$, there is a significant shift of the $\chi'$ peak temperature when the frequency of the AC magnetic field is modified. The corresponding K value is in the range observed for spin-glass metallic alloys such as *Cu*Mn or *Ag*Mn [40]. However $LaMn_{0.85}Ga_{0.15}O_3$ cannot be a true spin-glass phase since long-range magnetic order is observed by neutron diffraction. This 'spin-glass-like' behaviour around the Néel temperature is attributed to the competing antiferromagnetic and ferromagnetic

interactions present in the material. The same mechanism is probably also related to the especially high H* value ($\mu_0 H^*$ ~0.3T) encountered in the first magnetisation curve of the sample.

When the Ga substitution is increased, the antiferromagnetic component eventually disappears and gives way to a ferromagnetic ground state. In the case of the 50%Ga substitution, the saturation magnetic moment at low temperature (~3.7 $\mu_B$/Mn) almost reaches the spin-only theoretical value (4 $\mu_B$/Mn), despite the very substantial dilution of the $Mn^{3+}$-$Mn^{3+}$ interactions by the "non magnetic" gallium ions. However the temperature dependence of the in-phase AC susceptibility does not display the usual ferromagnetic behaviour. Below the Curie temperature (~ 57 K), the susceptibility decreases smoothly when the temperature decreases. Moreover, the position of the susceptibility maximum is influenced by the frequency of the AC magnetic field, with a K value close to that of $LaMn_{0.85}Ga_{0.15}O_3$. The fact that Cussen et al. [33] have found a long-range ferromagnetic order for $LaMn_{0.5}Ga_{0.5}O_3$ means that the magnetic ground state of this compound cannot be a single-phase spin-glass. However it is possible that the significant dilution of the $Mn^{3+}$ spins partially hinders the ferromagnetic ordering at very low magnetic field : the $\mu_0 H^*$ value found in the first magnetisation curve is only 0.035 T in the case of $LaMn_{0.5}Ga_{0.5}O_3$. In addition to the magnetic dilution effect, it must be kept in mind that, even though the long-range cooperative Jahn-Teller order is destroyed, a $Mn^{3+}$ ion in octahedral environment remains a Jahn-Teller ion, which means that dynamic and/or non-cooperative Jahn-Teller effects are still possible [6,22].

On the other hand, it can be noted that there is a systematic increase of the AC magnetic susceptibility when gallium ions are progressively substituted on the manganese site. This is true as well for the maximum susceptibility as for the low temperature values. On the whole, these results confirm the general trend of the $LaMn_{1-x}Ga_xO_3$ ($0 < x < 0.5$) system to evolve from A-type antiferromagnetism to a ferromagnetic ground-state.

The $LaMn_{0.85}Ni_{0.15}O_3$ also presents a ferromagnetic ground-state, as proved by the neutron diffraction results. However this compound is significantly different from the Ga-substituted compounds, especially concerning the electrical transport properties. Contrary to the latter samples, $LaMn_{0.85}Ni_{0.15}O_3$ exhibits smaller resistivity and activation energy than the reference compound $LaMnO_3$. Besides, a substantial magnetoresistance ratio is observed in the temperature range of the ferromagnetic transition.

This behaviour indicates that the nickel ions are mainly in the 2+ state (as recently confirmed by Sanchez et al. [41]) and that Ni substitution leads to the appearance of $Mn^{4+}$ charge carriers in the system. The combination of the ferromagnetic $Mn^{3+}$/$Mn^{4+}$ double exchange interactions with the dilution of the $Mn^{3+}$/$Mn^{3+}$ interactions results in a rapid destabilisation of the antiferromagnetic structure, as illustrated by the m(H) curve of the $LaMn_{0.85}Ni_{0.15}O_3$, which displays a typically ferromagnetic behaviour.

However the AC susceptibility behaviour is more intricate than that of a simple ferromagnetic compound. On decreasing the temperature, the paramagnetic-to-ferromagnetic transition corresponds to the usual rapid increase of the in-phase susceptibility, but $\chi'$ exhibits a noticeable decrease below ~ 90 K, before levelling off below ~ 65 K. The $\chi'$ drop corresponds to a peak in the $\chi''$ curve, and both features are shifted to higher temperatures when the frequency of the AC field is increased. The large

K value ($8.10^{-2}$) indicates a strong competition between different magnetic interactions, which could be expected considering that the system contains three different ions with unpaired electrons ($Mn^{3+}$, $Mn^{4+}$ and $Ni^{2+}$). However neutron diffraction shows long range magnetic order. It turns out that such an AC susceptibility behaviour is very similar to that of a $La_{0.9}Ca_{0.1}MnO_3$ sample studied by Joy et al. [42]. This compound has a $Mn^{4+}$ content close to that of $LaMn_{0.85}Ni_{0.15}O_3$ and that the characteristic temperatures ($T_C$ and "$T_{drop}$") are also very similar. These authors have attributed the low temperature decrease of the susceptibility to domain wall pinning effects. In the case of $LaMn_{0.85}Ni_{0.15}O_3$, it is possible that, at low temperature, the complexity of the spin interactions hinders the domain wall motion, which occurs through complicated spin rearrangements taking into account the competing magnetic exchange interactions.

## CONCLUSION

We have studied several samples obtained by substitution of gallium or nickel ions on the manganese site of $LaMnO_3$. In each case, we observed a progressive transition from the antiferromagnetic ordering of $LaMnO_3$ to a ferromagnetic-like ground state when the substitution level is increased. However, depending on the substituting cation ($Ga^{3+}$ or $Ni^{2+}$), different exchange mechanisms have to be considered, leading to noticeable differences in the physical properties (electrical transport, magnetic hysteresis,…).

Substitution by non-magnetic $Ga^{3+}$ ions progressively destroys the orbital ordering necessary for the antiferromagnetic order, leading to a ferromagnetic-like behaviour. It appears that this long-range ferromagnetic is retained even up to 50% substitution, despite the substantial dilution of the $Mn^{3+}/Mn^{3+}$ interactions. Ni substitution induces the appearance of ferromagnetic double exchange $Mn^{4+}/Mn^{3+}$ interactions competing with the $Mn^{3+}/Mn^{3+}$ super-exchange interactions. In addition, the $Ni^{2+}$ ions themselves take part into the exchange interactions, leading to a stabilisation of the ferromagnetic ground-state [12].

The AC susceptibility of these compounds was especially studied and interesting features have been observed, such as spin-glass-like sensitivity to the frequency of the AC magnetic field for samples displaying long range magnetic order detected by neutron diffraction. It appears that AC susceptibility is actually very sensitive to the existence of competing magnetic interactions in manganite compounds. In the future, it would be interesting to carry out systematic AC susceptibility studies in presence of superimposed DC magnetic fields [43], in order to probe the AC magnetic behaviour at different stages of the first magnetisation curve.

## ACKNOWLEDGEMENTS

B.V. is Scientific Research Worker of the F.N.R.S. (National Fund for Scientific Research) in Belgium. She thanks the European Commission for a Marie Curie Fellowship.

**REFERENCES**


[1] K. Chahara, T. Ohno, M. Kasai and Y. Kozono, Appl. Phys. Lett. 63 (1993) 1990.
[2] R. von Helmolt, J. Wecker, B. Holzapfel, L. Schultz and K. Samwer, Phys. Rev. Lett. 71 (1993) 2331.
[3] J. M. D. Coey, M. Viret and S. von Molnar, Adv. Phys. 48 (1999) 167.
[4] C. N. R. Rao, A. K. Cheetham and R. Manesh, Chem. Mater. 8 (1996) 2421.
[5] C. Zener, Phys. Rev. 82 (1951) 403.
[6] J. B. Goodenough, A. Wold, R. J. Arnott and N. Menyuk, Phys. Rev. 124 (1961) 373.
[7] K. Ghosh, S. B. Ogale, R. Ramesh, R. L. Greene, T. Venkatesan, K. M. Gapchup, R. Bathe and S. I. Patil, Phys. Rev. B 59 (1999) 533.
[8] R. Ganguly, I. K. Gopalakrishnan and J. V. Yakhmi, Physica B 275 (2000) 308.
[9] S. L. Yuan, Z. Y. Li, X. Y. Zeng, G. Q. Zhang, F. Tu, G. Peng, J. Liu, Y. Jiang, Y. P. Yang and C. Q. Tang, Eur. Phys. J. B 20 (2001) 177.
[10] C. N. R. Rao, A. Arulraj, P. N. Santhosh and A. K. Cheetham, Chem. Mater. 10 (1998) 2714.
[11] B. Raveau, A. Maignan, C. Martin and M. Hervieu, Chem. Mater. 10 (1999) 2641.
[12] S. Hebert, C. Martin, A. Maignan, R. Retoux, M. Hervieu, N. Nguyen and B. Raveau, Phys. Rev. B 65 (2002) 104420.
[13] K. Knizek, M. Daturi, G. Busca and C. Michel, J. Mater. Chem. 8 (1998) 1815.
[14] G. Biotteau, M. Hennion, F. Moussa, J. Rodriguez-Carvajal, L. Pinsard, A. Revcolevschi, Y. M. Mukovskii and D. Shulyatev, Phys. Rev. B 64 (2001) 104421.
[15] S. Uhlenbruck, R. Teipen, R. Klingeler, B. Büchner, O. Friedt, M. Hücker, H. Kierspel, T. Niemöller, L. Pinsard, A. Revcolevschi and R. Gross, Phys. Rev. Lett. 82 (1999) 185.
[16] J. Töpfer and J. B. Goodenough, J. Solid State Chem. 130 (1997) 117.
[17] A. K. Cheetham, C. N. R. Rao and T. Vogt, J. Solid State Chem. 126 (1996) 337.
[18] P. S. I. P. N. de Silva, F. M. Richards, L. F. Cohen, J. A. Alonso, M. J. Martinez-Lope, M. T. Casais, K. A. Thomas and J. L. MacManus-Driscoll, J. Appl. Phys. 83 (1998) 394.
[19] L. E. Gontchar, A. E. Nikiforov and S. E. Popov, J. Magn. Magn. Mater. 223 (2001) 1755.
[20] D. I. Khomskii and G. A. Sawatzky, Solid State Commun. 102 (1997) 87.
[21] Y. Tokura and Y. Tomioka, J. Magn. Magn. Mater. 200 (1999) 1.
[22] J. S. Zhou, H. Q. Yin and J. B. Goodenough, Phys. Rev. B 63 (2001) 184423.
[23] J. Töpfer and J. B. Goodenough, Eur. J. Solid State Inorg. Chem. 34 (1997) 467.
[24] J. Blasco, J. Garcia, J. Campo, M. C. Sanchez and G. Subias, Phys. Rev. B 66 (2002) 174431.
[25] B. Vertruyen, S. Hebert, A. Maignan, C. Martin, M. Hervieu and B. Raveau, Cryst. Eng. 5 (2002) 299.
[26] J. Blasco, J. Garcia, M. C. Sanchez, J. Campo, G. Subias and J. Perez-Cacho, Eur. Phys. J. B 30 (2002) 469.
[27] J. Blasco, M. C. Sanchez, J. Perez-Cacho, J. Garcia, G. Subias and J. Campo, J. Phys. Chem. Solids 63 (2002) 781.
[28] R. I. Dass, J. Q. Yan and J. B. Goodenough, Phys. Rev. B 68 (2003) 064415.

[29] V. L. Joly, P. A. Joy, S. K. Date and C. S. Gopinath, Phys. Rev. B 65 (2002) 184416.
[30] D. Flahaut, B. Vertruyen, C. Martin, S. Hébert, M. Hervieu, A. Maignan, B. Raveau, Z.Jirak, F. Bourée and G. André, in preparation.
[31] B. C. Hauback, H. Fjellvag and N. Sakai, J. Solid State Chem. 124 (1996) 43.
[32] J. B. Goodenough and J. M. Longo, Landoldt-Börnstein new series 4 (1970) 126.
[33] E. J. Cussen, M. J. Rosseinsky, P. D. Battle, J. C. Burley, L. E. Spring, J. F. Vente, S. J. Blundell, A. I. Coldea and J. Singleton, J. Am. Chem. Soc. 123 (2001) 1111.
[34] A. Maignan, C. Martin, G. Van Tendeloo, M. Hervieu and B. Raveau, Phys. Rev. B 60 (1999) 15214.
[35] J. S. Zhou and J. B. Goodenough, Phys. Rev. B 60 (1999) R15002-R15004.
[36] M. S. Kim, J. G. Park, K. H. Kim, T. W. Noh and H. C. Ri, J. Korean Phys. Soc. 37 (2000) 561.
[37] C. Ritter, M. R. Ibarra, J. M. De Teresa, P. Algarabel, C. Marquina, J. Blasco, J. Garcia, S. Oseroff and S. W. Cheong, Phys. Rev. B 56 (1997) 8902.
[38] B. Raveau, M. Hervieu, A. Maignan and C. Martin, J. Mater. Chem. 11 (2001) 29.
[39] E. Dagotto, T. Hotta and A. Moreo, Phys. Rep. 344 (2001) 1.
[40] J.A. Mydosh, Spin Glasses : An Experimental Introduction, Taylor & Francis, London, 1993.
[41] M. C. Sanchez, J. Garcia, J. Blasco, G. Subias and J. Perez-Cacho, Phys. Rev. B 655 (2002) 144409.
[42] P. A. Joy and S. K. Date, J. Magn. Magn. Mater. 220 (2000) 106.
[43] Ph. Vanderbemden, B. Vertruyen, A. Rulmont, R. Cloots, G. Dhalenne and M. Ausloos, Phys. Rev. B 68 (2003) 224418.

## FIGURE CAPTIONS

**Fig. 1.** Room temperature X-ray diffraction patterns for the different samples.

**Fig. 2.** Cell parameters (full symbols) and cell volume (empty circles) for the different samples (Pnma space group)

**Fig. 3.** Temperature dependence of the AC susceptibility in-phase component for $LaMnO_3$ and the gallium-substituted samples for $\mu_0 H_{AC}$ = 1 mT and f = 100, 1000 and 10000 Hz.

**Fig. 4.** Temperature dependence of the in-phase ($\chi'$) and out-of-phase ($\chi''$) components of the AC susceptibility of the $LaMn_{0.85}Ni_{0.15}O_3$ sample for $\mu_0 H_{AC}$ = 1 mT and f = 100 and 1000 Hz.

**Fig. 5.** DC magnetic field dependence of the magnetic moment at 5 K for the different samples between –5 and + 5 T. The magnetic moment values are given in $\mu_B$/formula unit.

**Fig. 6.** First-magnetisation curves at 5 K for $LaMn_{0.85}Ga_{0.15}O_3$ (main figure) and $LaMn_{0.85}Ni_{0.15}O_3$ (inset). The magnetic moment values are given in $\mu_B$/formula unit. The arrow corresponds to the characteristic field H*, as explained in the text.

**Fig. 7.** Temperature dependence of the electrical resistivity of the different samples. Note the logarithmic resistivity scale.

**Table 1** : Comparison of the characteristic parameters of some thermal, electrical and magnetic properties measured on the different samples, as explained in the text.

| | $LaMnO_3$ | $LaMn_{0.85}Ga_{0.15}O_3$ | $LaMn_{0.5}Ga_{0.5}O_3$ | $LaMn_{0.85}Ni_{0.15}O_3$ |
|---|---|---|---|---|
| $S_{300\,K}$ ($\mu$V/K) | 460 | 355 | | 175 |
| K (see text) | $4.10^{-4}$ | $5.10^{-3}$ | $7.10^{-3}$ | $8.10^{-2}$ |
| m($\mu_B$/fu) at 5 K and 5 T | 0.37 | 1.33 (1.56 $\mu_B$/Mn) | 1.86 (3.72 $\mu_B$/Mn) | 3.46 |
| Coercive field $\mu_0 H_c$ (T) at 5K | 0.85 | 0.6 | 0.05 | < 0.01 |
| Remnant magnetisation $m_r$ ($\mu$B/fu) at 5 K | 0.1 | 0.5 (0.6 $\mu_B$/Mn) | 0.5 (1 $\mu_B$/Mn) | 0.2 |
| $\mu_0 H^*$(T) (see text) | 0.1 | 0.3 | 0.035 | < 0.01 (if any) |
| $E_a$ (meV) | 220 | 220 | 260 | 140 (T > 170K) 120 (T < 170K) |
| $\rho_{350\,K}$ ($\Omega$.cm) | 34 | 60 | 1100 | 1.8 |

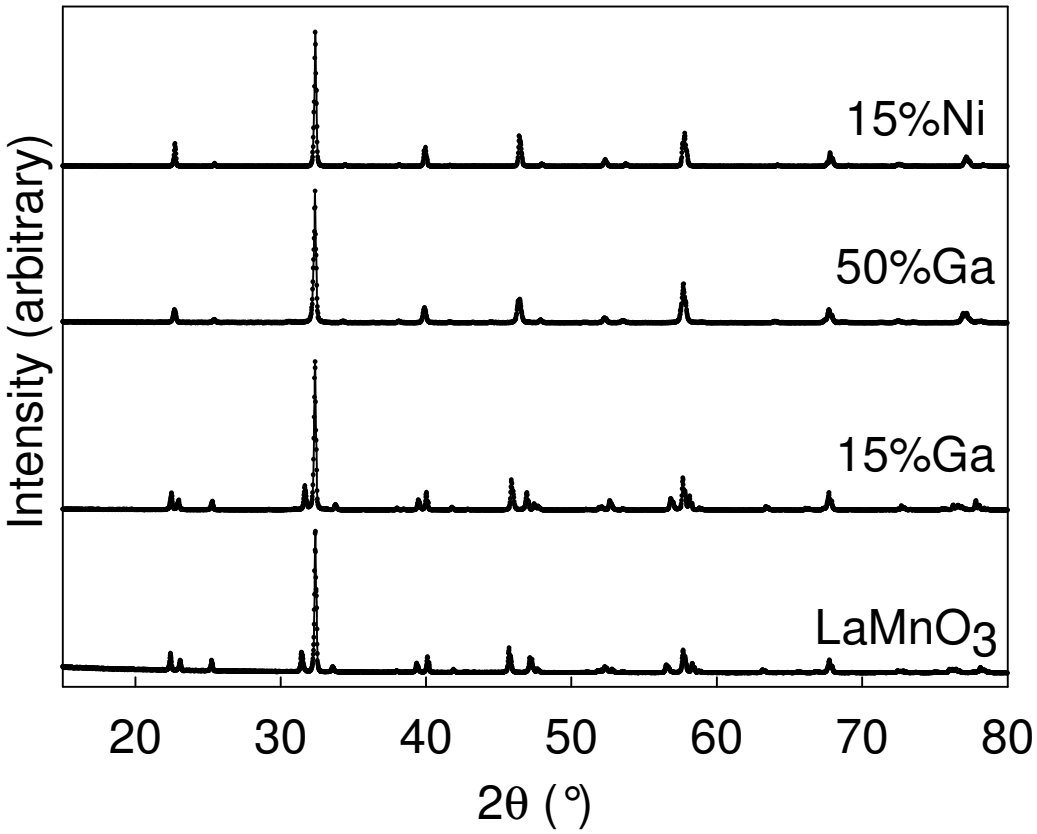
15%Ni
50%Ga
15%Ga
LaMnO3
Intensity (arbitrary)
20
30
40
50
60
70
80
2θ (°)

Figure 1

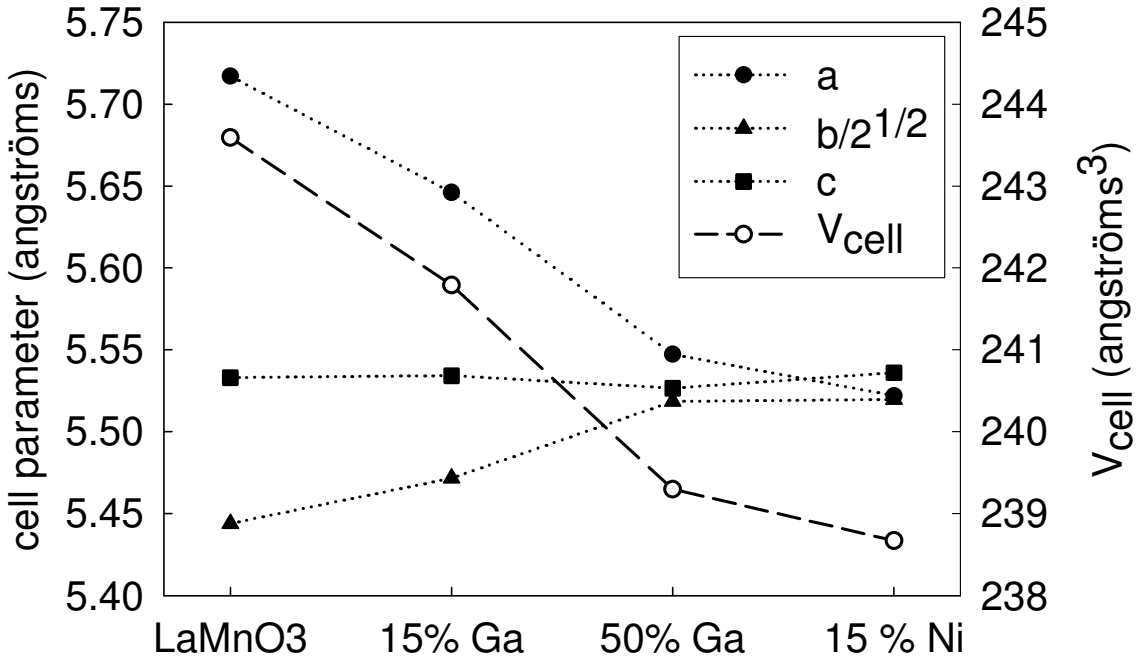
5.75
5.70
5.65
5.60
5.55
5.50
5.45
5.40
cell parameter (angströms)
245
244
243
242
241
240
239
238
Vcell (angströms3)
a
b/21/2
c
Vcell
LaMnO3
15% Ga
50% Ga
15 % Ni

Figure 2

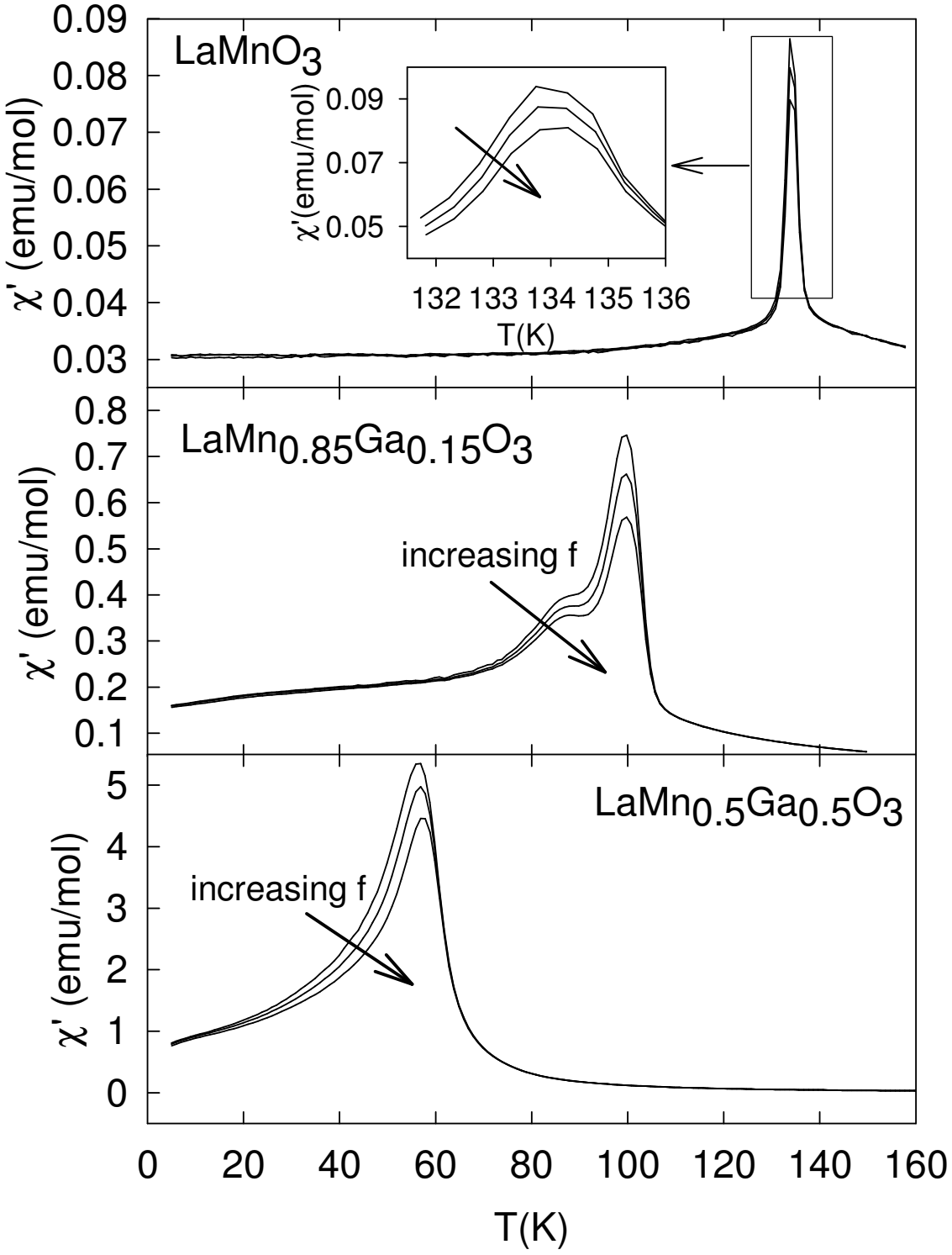
LaMnO3
χ' (emu/mol)
0.09
0.08
0.07
0.06
0.05
0.04
0.03
χ'(emu/mol)
0.09
0.07
0.05
132 133 134 135 136
T(K)
LaMn0.85Ga0.15O3
increasing f
0.8
0.7
0.6
0.5
0.4
0.3
0.2
0.1
LaMn0.5Ga0.5O3
increasing f
5
4
3
2
1
0
0 20 40 60 80 100 120 140 160
T(K)

Figure 3

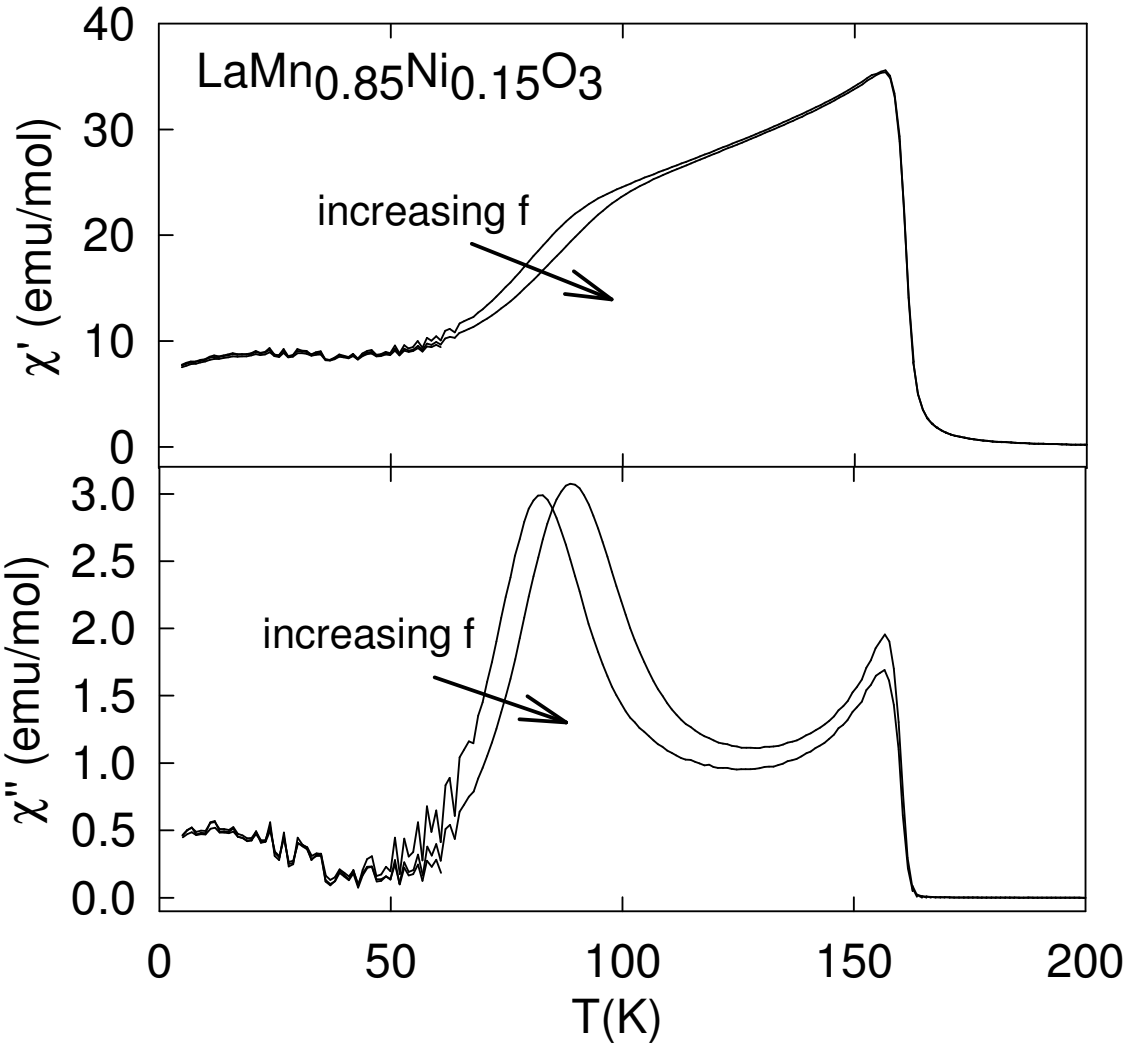
LaMn0.85Ni0.15O3
increasing f
χ' (emu/mol)
increasing f
χ'' (emu/mol)
T(K)
0
10
20
30
40
0.0
0.5
1.0
1.5
2.0
2.5
3.0
0
50
100
150
200

Figure 4

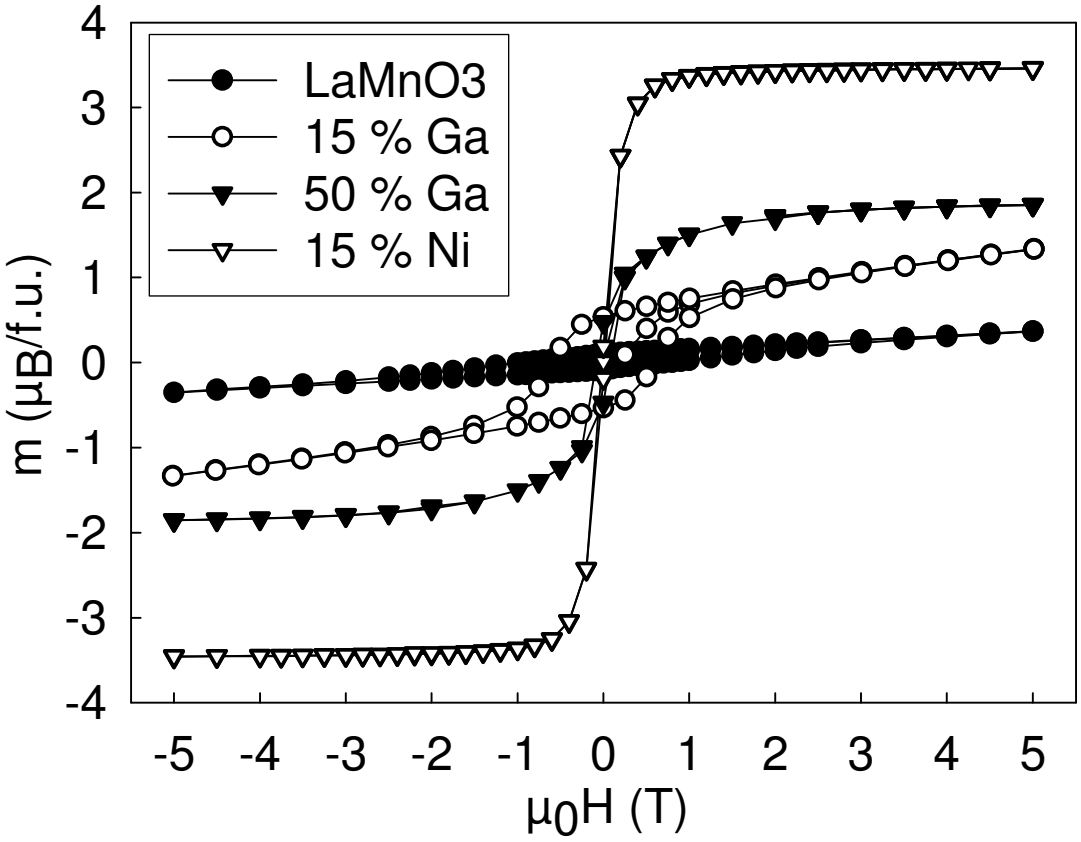


Figure 5

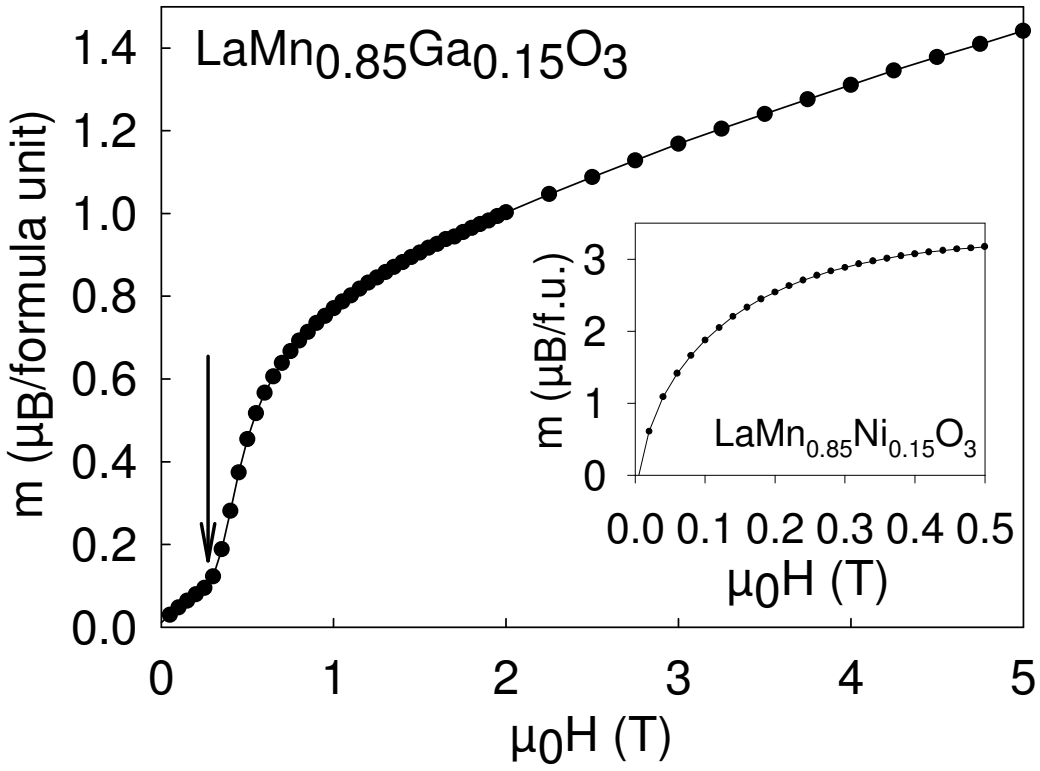
LaMn0.85Ga0.15O3
m (μB/formula unit)
μ0H (T)
LaMn0.85Ni0.15O3
m (μB/f.u.)
μ0H (T)

Figure 6

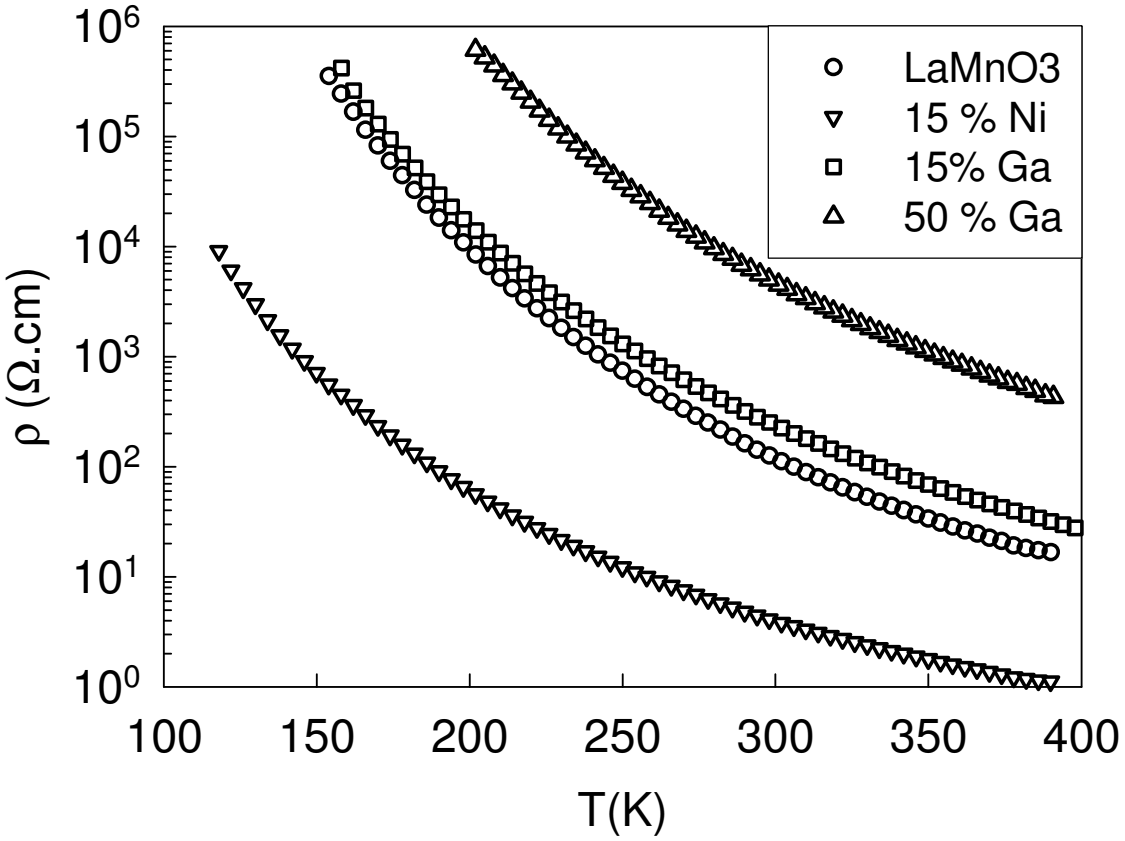
LaMnO3
15 % Ni
15% Ga
50 % Ga
ρ (Ω.cm)
T(K)
10^6
10^5
10^4
10^3
10^2
10^1
10^0
100
150
200
250
300
350
400

Figure 7